Design of Novel TDOF Nonlinear PID Controllers for Linear and Nonlinear Systems*

Gun-Baek SO[1], Gang-Gyoo JIN[2], Yung-Deug SON[3]*

[1] Department of Maritime Industry Convergence, Mokpo National Maritime University,
91 Haeyangdaehak-ro, Mokpo 58628, Republic of Korea
sgb@mmu.ac.kr

[2] Department of Information and Communication, Huree College of ICT, Bayanzurkh District,
13th Khoroo, Ulaanbaatar 16061, Mongolia
gjin30@gmail.com

[3] Department of Mechanical Facility Control Engineering, Korea University of Technology and Education,
1600 Chungjeol-ro, Dongnam-gu, Cheonan 31253, Republic of Korea
ydson@koreatech.ac.kr (**Corresponding author*)

Abstract: Proportion-Integral-Derivative (PID) controllers are widely used for process control across various industries, including the chemical industry. However, the traditional one-degree-of-freedom PID controller struggles to balance a good setpoint tracking and disturbance rejection. This paper proposes two novel two-degree-of-freedom nonlinear PID (TDOF NPID) controllers. As such, this approach combines a nonlinear PID controller with its specific strengths with an independent linear compensator, which can be either a P-type or a PD-type compensator. A hybrid genetic algorithm is also employed for optimizing the parameters of the TDOF nonlinear PID controllers, considering both the setpoint tracking and disturbance rejection performance, with the goal of minimizing the integral of absolute error criterion. The performance of the proposed controllers is evaluated by benchmarking them against the traditional PID controller for three processes with varying orders and one nonlinear system.

Keywords: Nonlinear PID controller, Two-degree-of-freedom, Feedforward compensator, Parameter tuning, Hybrid genetic algorithm.

1. Introduction

The proportional-integral-derivative (PID) controllers have been widely adopted in various control loops due to their simple structure, their ease of design and tuning, and the field technicians` familiarity with them. One-degree-of-freedom (ODOF) PID controllers, despite their popularity, exhibit limitations in balancing multiple objectives due to their one degree of freedom. When tuning focuses on setpoint tracking, disturbance rejection is affected, and vice versa. For this reason, they are typically tuned for a single objective, such as good setpoint tracking or good disturbance rejection, and operated to suit one purpose. Various tuning methods for ODOF PID controllers have been reported in the literature, including heuristic methods, stability analysis methods (Wu et al., 2016), linear quadratic regulator (LQR) methods (Sundari & Nachiappan, 2018), internal model control (IMC) methods (Shamsuzzoha, 2013), and direct synthesis (DS) methods (Chen & Seborg, 2002).

However, in many real-world applications, such as airplane and ship autopilots, room temperature control, chemical process control, and vehicle cruise control, there may be multiple objectives that need to be balanced, such as tracking and regulation. In this regard, it may be hard for traditional PID controllers to find settings that effectively address both. To approach this limitation of traditional PID controllers, researchers have proposed various advancements in the literature. Some studies have focused on incorporating artificial intelligence techniques like fuzzy logic (Allagui et al., 2021) and neural networks (Goh et al., 2017), or using adaptive control (Mahmooddabadi et al., 2014; Hasan & Abbas, 2022) and model predictive control (Santos & Raffo, 2016; Zou & Li, 2015).

Mahmooddabadi et al. (2014) proposed an adaptive robust PID control using a genetic algorithm and supervisory decoupled sliding mode control to address the limitations of the linear PID control, achieving an optimal control performance and resolving the chattering issue. Hasan & Abbas (2022) proposed an adaptive nonlinear PID controller to address the path-tracking problem for a 6-degree-of-freedom (6-DOF) underwater

* This paper is an extended study of a previous paper with the title "Design of a Nonlinear PID Controller and Tuning Rules for First-Order Plus Time Delay Models", published in Studies in Informatics and Control journal, vol. 28(2), 2019, pp. 157–166 (DOI: 10.24846/v28i2y201904).

robotic vehicle (URV) model, which demonstrated an improved performance in comparison with the conventional nonlinear PID controller.

A constrained model predictive controller (MPC) was presented in literature to solve the path tracking problem of a Tilwas t-rotor UAV carrying a suspended load. The simulation results demonstrated that the proposed MPC effectively reduced the load's swing and achieved an excellent path tracking performance (Santos & Raffo, 2016). In (Zou & Li, 2015), the authors proposed a new PI-PD method optimized by an extended non-minimal state space model predictive control to address the issues of nonlinearity, uncertainty, and large time delays. This method demonstrated a superior performance in comparison with various traditional PID controllers.

Several research efforts have addressed the challenge of incorporating nonlinearities into PID control schemes. There are two main approaches for handling nonlinearities: nonlinear error scaling and employing nonlinear functions to control the gains directly (Zhang & Hu, 2012; Chen et al., 2011; Sun et al., 2022). With regard to the former approach for handling nonlinearities, Seraji (1998) used sigmoid and hyperbolic functions for scaling, while Jiang & Gao (2001) implemented a nonlinear PID (NPID) controller for an anti-lock braking system with error scaling. Jin & Son (2019) proposed a NPID controller specifically designed for first-order plus time delay (FOPTD) models. This controller builds on the traditional PID structure, but incorporates a nonlinear gain element to scale the error signal of the integral term. The authors proposed three practical tuning rules for this NPID controller. For the latter approach for handling nonlinearities, Zhang & Hu (2012) introduced a NPID controller for a generator's excitation control system. The controller employs a unique gain structure utilizing hyperbolic secant and exponential functions. A control approach was investigated for an electro-hydraulic servo system in (Chen et al., 2011). They implemented nonlinear proportional and integral actions by taking the square of the error as input, and implemented a nonlinear differential gain using an exponential function of the error. This resulted in an improved performance in comparison with traditional PI controllers. In (Sun et al., 2022), the authors proposed a NPID Controller for CNC Systems, where the nonlinear gains were directly implemented using hyperbolic secant and exponential functions. So, the proportional and integral gains were implemented with hyperbolic secant functions, while the derivative gain was implemented with an exponential function (Wang et al., 2009).

Some studies have also been conducted on extending the capabilities of linear PID controllers by adding one more degree of freedom. The concept of two-degree-of-freedom (TDOF) PID controller was coined by Araki (1984) in the mid 1980s as a way to address the limitations of traditional ODOF PID controllers. TDOF PID controllers overcome these limitations by providing two degrees of freedom, which allows for more flexibility in tuning the controller. This flexibility can be used to improve the controller's performance in terms of setpoint tracking (trajectory following) and disturbance rejection (regulation). Pathiran (2019) proposed a TDOF controller using PID control and IMC to improve both setpoint tracking and disturbance rejection, and demonstrated its superior performance for first-order and second-order processes with time delays. Santosh Kumar & Padma Sree (2016) proposed a TDOF controller consisting of an IMC-based PIDC controller and a setpoint filter to control various integrating processes with time delays. TDOF controllers for various integrating systems with time delays were proposed, where the main controller, either PID or PIDC, was designed based on the DS approach, and a setpoint filter was used to enhance the setpoint tracking performance. A DS-based TDOF controller is proposed for the temperature control of the regasification system for LNG-fueled marine engines, and for controlling a pure integrating process with time delay in (So, 2022).

Many real-world systems, such as industrial robots, autonomous vehicles, aircraft, and chemical plants, require both an accurate trajectory tracking and disturbance rejection. While integral action in PID controllers effectively eliminates the steady-state error, it can lead to overshoot, oscillations, and integral windup during sudden setpoint and/or disturbance changes. To address

these limitations, this research proposes two novel TDOF NPID controllers that utilize either a P-type or PD-type feedforward compensator to augment the NPID controller proposed by Jin & Son (2019). The hybrid genetic algorithm (HGA) presented by Jin & Jarso (2024) is used for tuning the parameters of the TDOF NPID controllers. To assess controller performance, the integral of absolute error criterion is minimized. The effectiveness of the proposed controllers is compared with that of the PID controller for three different processes and one nonlinear system.

The remainder of this paper is organized as follows. Section 2 briefly describes the existing linear PID and NPID controllers that are used for comparison purposes. Section 3 presents the framework for designing the two TDOF NPID controllers and for tuning the controller parameters. Subsequently, Section 4 validates the effectiveness of the proposed methods through simulation involving their related processes. Finally, Section 5 concludes this paper and outlines a future research direction.

2. Existing PID Controllers

In this section, two different types of PID controllers are reviewed.

2.1 Practical PID Controller

The ideal derivative term of the conventional PID controller can amplify high-frequency noises or abrupt setpoint changes and/or disturbance changes in control loops. This can lead to an undesirable phenomenon called *Derivative Kick*. To avoid this, most PID controllers in the field use a filter on the derivative term for a smoother control (Raja & Ali, 2021). The transfer function of the practical PID controller with a filter is given by:

$$G_{pid}(s) = K_p + \frac{K_i}{s} + K_d D(s) \tag{1a}$$

$$D(s) = \frac{s}{1 + \frac{T_d}{N} s} \tag{1b}$$

where K_p, K_i and K_d are the proportional, integral, and derivative gains, respectively. $T_d = K_d / K_p$ denotes the derivative time. $D(s)$ is an approximation of the ideal differentiator and N is a user-defined parameter. The magnitude of its frequency, namely $K_d \mid D(j\omega) \mid = K_d \omega / \sqrt{1 + T_d^2 \omega^2 / N^2}$ is limited to NK_p as $\omega \to \infty$. This means that high-frequency measurement noise is amplified at most by a factor NK_p. N is appropriately selected to achieve the desired filtering effect and the typical values of N range from 5 to 30 (Åström et al., 1998). For the purpose of this study, N is set at 10. It should be noted that if $N \to \infty$, $D(s)$ becomes the ideal differentiator.

2.2 Nonlinear PID Controller

Linear PID controllers ensure a superior performance when operating near the designated areas. However, as the process dynamics changes or becomes unpredictable, their performance can degrade significantly. For processes with nonlinear characteristics, one alternative is to use NPID controllers that bring benefits like a smoother operation and better handling of unexpected changes. However, designing and setting up NPID controllers is more complex than designing and setting up linear PID controllers, as they involve more tuning parameters (Jin & Son, 2019; Sun et al., 2022).

Jin & Son (2019) proposed a NPID controller, extending the traditional PID framework. This NPID controller requires only three tuning parameters. To address the limitations of the traditional PID controller's integral action, which can lead to overshoot, oscillations, and integral windup during dynamic conditions, the NPID controller introduces a nonlinear gain. This nonlinear gain dynamically scales the error signal fed into the integrator, improving the controller's response to sudden changes in setpoint and disturbances. Its time-domain is given by:

$$\begin{aligned} u(t) &= u_p(t) + u_i(t) + u_d(t) \\ u_p(t) &= K_p e(t) \\ u_i(t) &= K_i \int \varsigma(t) dt \\ \frac{T_d}{N} \frac{du_d(t)}{dt} + u_d(t) &= K_d \frac{de(t)}{dt} \end{aligned} \tag{2}$$

where u_p, u_i and u_d denote the proportional, integral and derivative actions, respectively and $\varsigma(t)$ is the scaled error given by:

$$\varsigma(t) = k(e) e(t) \tag{3}$$

$k(e)$ in equation (3) represents a nonlinear gain of

$$k(e) = \exp(-\frac{e^2}{2\sigma^2}) \tag{4}$$

where σ represents the biggest change in the setpoint value between steps.

Figure 1 shows the graphical representation of $\varsigma(t)$ for typical values of σ of 1, 2 and 3.

This error scaling allows for a reduction of the accumulated error during periods of large error (anticipating potential overshoot and oscillations) and an increase during periods of smaller error (to maintain steady-state error reduction).

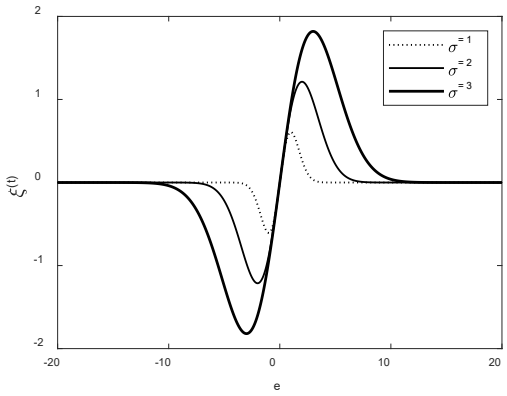

Figure 1. Graphical representation of $\varsigma(t)$ for typical values of σ of 1, 2 and 3

The transfer functions of the linear part of the NPID controller are:

$$G_{pd}(s) = \frac{U_{pd}(s)}{E(s)} = K_p + K_d D(s) \tag{5a}$$

$$\frac{U_i(s)}{Z(s)} = \frac{K_i}{s} \tag{5b}$$

where $D(s)$ is the same as $D(s)$ used in equation (1b). Figure 2 depicts the NPID control system. A disturbance signal, denoted by d, is applied to the input side of the system. In the block diagram, y_s is the setpoint, y the output, e the error between the setpoint and the output and u the control input.

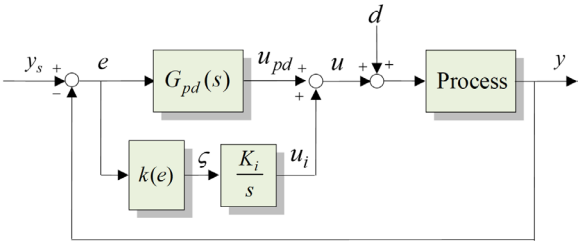

Figure 2. Block diagram of the NPID control system

While the previously mentioned NPID controller offers advantages over the linear PID controller, it remains an ODOF controller. This inherent limitation restricts its ability to perfectly balance improvements in both setpoint tracking and disturbance rejection.

3. Proposed TDOF NPID Controllers

This section introduces two new controllers that use the TDOF and NPID techniques.

3.1 NPID Controller with a PD-type Feedforward Compensator

As mentioned before, one of the limitations of ODOF PID controllers is that they cannot simultaneously improve setpoint tracking and disturbance rejection. Improving the setpoint tracking capability decreases the disturbance rejection capability, and vice versa.

A wide range of real-world systems, including industrial robots, autonomous vehicles, aircraft, and chemical plants, require the system's good response to both reference inputs and disturbances. To address this dual requirement, TDOF control can be strategically incorporated into either feedforward or feedback control paths. One of the popular choices for industrial applications is the use of TDOF control in a feedforward path. A TDOF NPID control scheme with a feedforward compensator is proposed in this paper as shown in Figure 3.

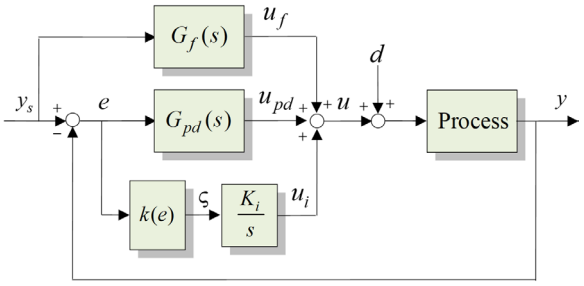

Figure 3. TDOF NPID control system with a feedforward compensator

A form of PD-type feedforward compensator is the one proposed by Araki & Taguchi (2003) as:

$$G_f(s) = -K_p[\alpha + \beta T_d D(s)] \tag{6}$$

where α and β are the setpoint weights on the proportional term and the derivative term, respectively. $D(s)$ is the same as in equation (1b). The TDOF NPID controller illustrated in Figure 2 can overcome the limitations of ODOF linear

or nonlinear PID controllers by providing one additional degree of freedom which allows for more flexibility in tuning the controller. After manipulating the equations (5a) and (6), the linear parts of the TDOF NPID controller can be expressed as equation (7):

$$\begin{aligned} U_{pd}(s)+U_f(s) &= G_{pd}(s)E(s)+G_f(s)Y_s(s) \\ &= K_p[1+T_dD(s)][Y_s(s)-Y(s)] \\ &\quad -K_p[\alpha+\beta T_dD(s)]Y_s(s) \\ &= K_p[(1-\alpha)Y_s(s)-Y(s)] \\ &\quad +K_pT_dD(s)[(1-\beta)Y_s(s)-Y(s)] \end{aligned} \tag{7}$$

Then, the equivalent block diagram is redrawn as shown in Figure 4.

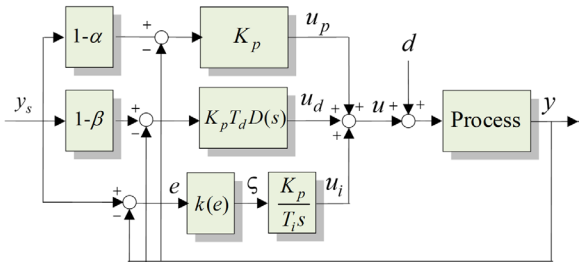

Figure 4. Equivalent TDOF NPID control system with a PD-type feedforward compensator

By examining this equivalent transformation, one can gain a deeper understanding of how the TDOF structure influences various aspects of the system. This controller features five adjustable parameters (K_p, K_i, K_d, α and β) for tuning its dynamic response.

3.2 NPID Controller with a P-type Feedforward Compensator

As it can be seen in equation (6) and Figure 3, by including an additional degree of freedom, the TDOF NPID controller has two more adjustable parameters then the existing ODOF PID controllers. This may become a burden for field engineers. In this case, a NPID controller with a P-type feedforward compensator can be a compromise between performance enhancement and tuning burden as expressed in:

$$G_f(s) = -\alpha K_p \ (\beta = 0) \tag{8}$$

Figure 5 shows the structure of the NPID controller with a P-type feedforward compensator.

This controller has four tuning parameters (K_p, K_i, K_d, and α). To simplify subsequent discussions, the TDOF NPID controller using the PD-type feedforward compensator in equation (6) will be denoted as the TDOF-NPID2 controller. Similarly, the TDOF NPID controller with the P-type feedforward compensator in equation (8) will be denoted as the TDOF-NPID1 controller.

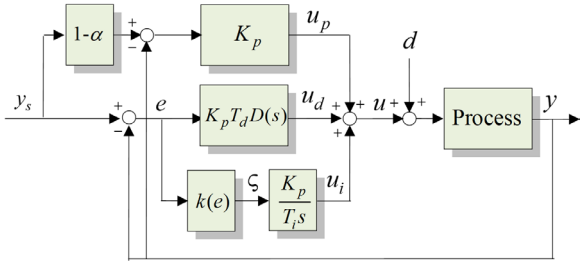

Figure 5. TDOF NPID control system with a P-type feedforward compensator

3.3 Tuning of the TDOF NPID Controllers

The tuning of the two controllers presented in the previous subsections reveals the optimal parameters $\boldsymbol{p}_1 = [K_p, K_i, K_d, \alpha]^T \in \boldsymbol{S}$ for the TDOF-NPID1 controller and $\boldsymbol{p}_2 = [K_p, K_i, K_d, \alpha, \beta]^T \in \boldsymbol{S}$ for the TDOF-NPID2 controller, where $\boldsymbol{S} = \{\boldsymbol{p}_i \in \Re^3 \text{ or } \Re^4 | \ \boldsymbol{p}_i^{(L)} \le \boldsymbol{p}_i \le \boldsymbol{p}_i^{(U)}, \ i = 1,2\}$ is the search space, and $\boldsymbol{p}_i^{(L)}$ and $\boldsymbol{p}_i^{(U)}$ are the lower and upper bounds, respectively. Optimizing this problem requires defining a performance metric and using an algorithm to find the setting that minimizes it.

3.3.1 Performance Metrics

Adjusting a controller's settings impacts both its responsiveness to the desired setpoint and its ability to manage disturbances. These two settings are often in conflict. This trade-off is explored by simulating a FOPTD process, $Ke^{-Ls}/(1+Ts)$ with a gain (K) of 1, a dimensionless L/T ratio, and a parameter (N) of 10 for the controllers. To evaluate the controller's performance, common measures like the integral absolute error (*IAE*) are used.

$$IAE_{SP} = \int_0^\infty |\, y_s(t) - y(t) \,|\, dt \tag{9a}$$

$$IAE_{DIS} = \int_0^\infty |\, y(t) \,|\, dt \tag{9b}$$

where IAE_{SP} is a measure of the error between the setpoint and the output over time while applying $y_s = 1$ and $d = 0$, and IAE_{DIS} is the same measure while applying $y_s = 0$ and $d = 1$. For the NPID controllers, $\sigma = 1$ is utilized.

The non-dominated sorting genetic algorithm (NSGA-II) (Deb et al., 2002) was applied for minimizing the two performance metrics above simultaneously for three distinct L/T ratio values, namely 0.1, 0.5 and 1. Figure 6 shows the optimal Pareto fronts.

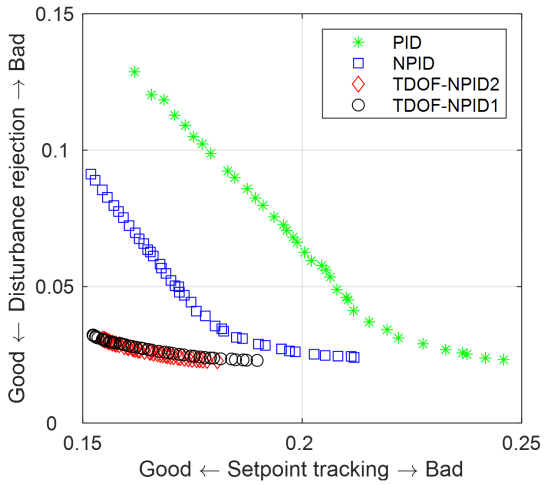

(a) $L/T = 0.1$

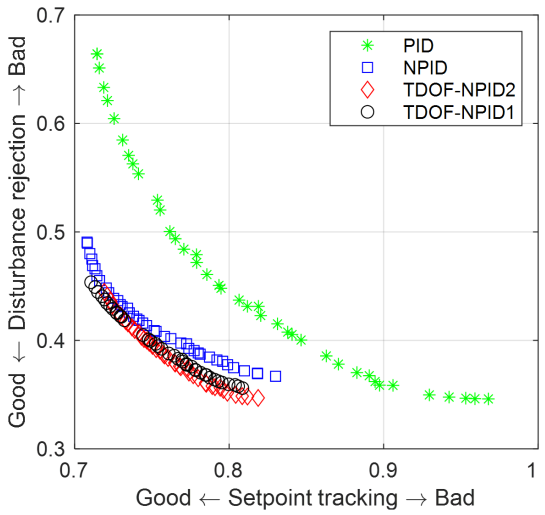

(b) $L/T = 0.5$

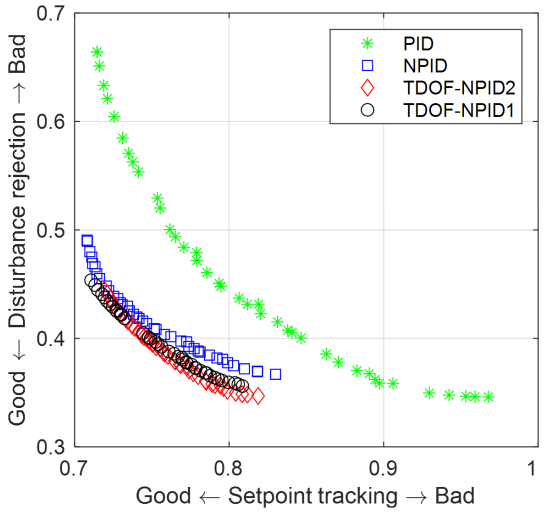

(c) $L/T = 1$

Figure 6. Optimal Pareto fronts

There is an inherent conflict between achieving a good setpoint tracking and a strong disturbance rejection, as shown in Figure 6. Prioritizing one performance metric comes at the expense of the other. The following facts can be drawn:

- The linear PID controller lags behind the other three controllers in terms of its overall performance. In other words, all NPID controllers outperform the linear PID controller;
- In particular, the smaller the value of L/T, the better the overall performance of the NPID controllers in comparison with the linear PID controller;
- Although the TDOF-NPID2 controller features a better performance than the TDOF-NPID1 controller by introducing an extra parameter, the difference is small.

Building on the findings of this analysis, the TDOF NPID controllers are optimized. To strike a balance between the two settings, a single performance metric derived from equation (9) is employed:

$$IAE = IAE_{SP} + w \cdot IAE_{DIS} \tag{10}$$

where w is a weighting coefficient that determines the relative importance of two different criteria to maximize the overall performance of the proposed controllers across all criteria. Increasing the weight of one performance measure might necessitate to reduce the weight of another performance measure. For this study, w is set at 1. However, w may vary across different control environments.

3.3.2 Optimization Algorithm

To find the solution to this optimization problem, a hybrid genetic algorithm (HGA) is employed that relies on two primary operators: affine combination-based reproduction and non-uniform mutation (Jin & Jarso, 2024). The pseudo code of the HGA is given below:

Algorithm.

Set $t = 0$;
Create an initial population of individuals of length L;
Evaluate the function value $f_i(t)$ of each individual;
Determine the local best and worst function values ($f_{best}(t)$, $f_{worst}(t)$) in the population and set the global best ($\boldsymbol{x}_{global}(t)$, $f_{global}(t)$).
At $t = 0$, the global best becomes the local best;
while (termination is not met) do the following steps
    Set $t = t+1$;
    Apply the affine combination-based reproduction;
    Apply the non-uniform mutation;
    Evaluate the function value $f_i(t)$ of each individual;
    Determine the local best and worst function values ($f_{best}(t), f_{worst}(t)$) in the population and update the global best ($\boldsymbol{x}_{global}(t), f_{global}(t)$). If the local best is better than the global best, then it becomes the new global best;
end while

4. Simulation Results

This section evaluates the performance of the TDOF-NPID1 and TDOF-NPID2 controllers using three processes with varying orders and the parameter c (Veronesi & Visioli, 2023) and one nonlinear system (Sprott, 2000; Rosas Almeida et al., 2006). The proposed controllers are compared with the PID controller. To ensure a fair comparison, the PID controller is also optimized using the HGA to achieve the same goal: minimizing the performance index defined in equation (10). Several metrics are used for evaluating the performance of all three methods with regard to setpoint tracking and disturbance rejection. For setpoint tracking, the overshoot M_p of 5%, the settling time t_s and the integral of absolute error IAE_{SP} are measured. For disturbance rejection, the perturbance peak M_{peak}, recovery time t_{rcy}, and IAE_{DIS} are measured. M_{peak} can be expressed as $|y_{max}-y_s|$ or $|y_{min}-y_s|$ and t_{rcy} determines the duration for y to recover to a value within 2% of the setpoint.

4.1 Case 1: First-order Plus Time Delay Process

A first-order process with two distinct time delays of 0.5 and 4 is considered as:

$$G_1(s) = \frac{1}{1+5s}e^{-cs},\ c = 0.5, 4 \qquad (11)$$

The settings for the three controllers, optimized using the HGA, are shown in Table 1 for each value of c.

Figures 7 and 8 show the setpoint tracking responses to unit step input and the disturbance rejection responses to unit step disturbance for the three controllers for process 1 and the two values of the parameter c. It can be seen that the TDOF NPID controllers give better responses with a smaller overshoot than the PID controller. Further on, a comparison of the two TDOF NPID controllers reveals that the TDOF-NPID2 controller gives slightly better responses.

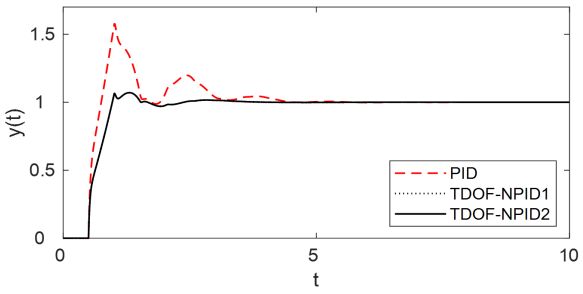

(a) Setpoint tracking

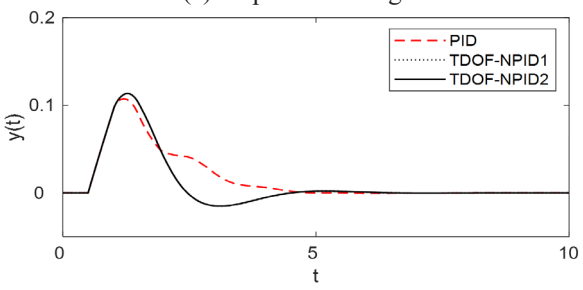

(b) Disturbance rejection

Figure 7. Responses of the three controllers for process 1 with c = 0.5

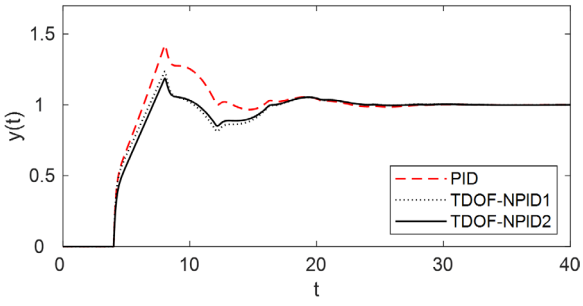

(a) Setpoint tracking

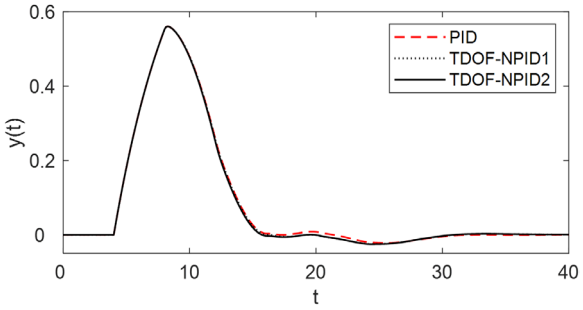

(b) Disturbance rejection

Figure 8. Responses of the three controllers for process 1 with c = 4.0

Table 1. Tuned parameters of the three controllers for process 1

c	Controller	Parameters				
		K_p	K_i	K_d	α	β
0.5	PID	10.051	6.352	2.920	-	-
	TDOF-NPID1	9.415	9.431	2.104	0.323	-
	TDOF-NPID2	9.426	9.435	2.108	0.322	0.005
4	PID	1.521	0.298	2.307	-	-
	TDOF-NPID1	1.517	0.333	2.270	0.069	-
	TDOF-NPID2	1.528	0.336	2.303	0.095	0.191

Table 2. Performance comparison for the three controllers for process 1

c	Controller	Setpoint tracking			Disturbance rejection		
		M_p	t_s	IAE_{SP}	M_{peak}	t_{rcy}	IAE_{DIS}
0.5	PID	57.8845	2.9543	1.0137	0.1072	4.0992	0.1590
	TDOF-NPID1	7.0183	1.4283	0.7260	0.1134	3.9832	0.1436
	TDOF-NPID2	7.0493	1.4289	0.7265	0.1134	3.9809	0.1433
4	PID	42.0755	19.6993	6.3219	0.5602	14.9615	3.6078
	TDOF-NPID1	23.5261	19.7430	5.9877	0.5603	14.9092	3.6289
	TDOF-NPID2	18.6655	19.7788	5.9855	0.5602	14.7934	3.6041

Table 2 summarizes the results related to the performance of the three controllers for a quantitative comparison for Process 1. It is evident from Table 2 that in comparison with the PID controller, the overshoot M_p, the settling time t_s, and IAE_{SP} of the TDOF NPID controllers are smaller.

For disturbance rejection, the M_{peak} obtained by all the employed methods is similar, but the TDOF NPID controllers obtained a shorter t_{rcy} than the PID controller, with the IAE_{DIS} of the TDOF-NPID2 controller being the lowest.

4.2 Case 2: Second-order Plus time Delay Process

A second-order process with a time delay is considered. The process parameter c has two distinct values, namely 2 and 5.

$$G_2(s) = \frac{1}{(1+cs)^2} e^{-s}, \; c = 2, 5 \qquad (12)$$

Table 3 shows the settings for the three controllers used in this process, each optimized for the two values of c.

Table 3. Tuned parameters of the three controllers for process 2

c	Controller	Parameters				
		K_p	K_i	K_d	α	β
2	PID	2.724	0.887	3.117	-	-
	TDOF-NPID1	2.660	1.124	3.082	0.080	-
	TDOF-NPID2	3.207	1.289	3.601	0.214	0.483
5	PID	7.220	1.166	15.185	-	-
	TDOF-NPID1	5.724	2.083	14.208	0.241	-
	TDOF-NPID2	9.351	2.848	16.773	0.338	0.506

Figures 9 and 10 show the setpoint tracking responses to unit step input and the disturbance rejection responses to unit step disturbance for the three controllers for process 2 and the two respective values of the parameter c. Table 4 quantitatively compares the performance of these controllers on Process 2.

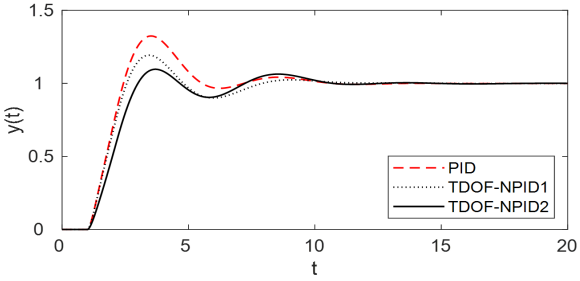

(a) Setpoint tracking

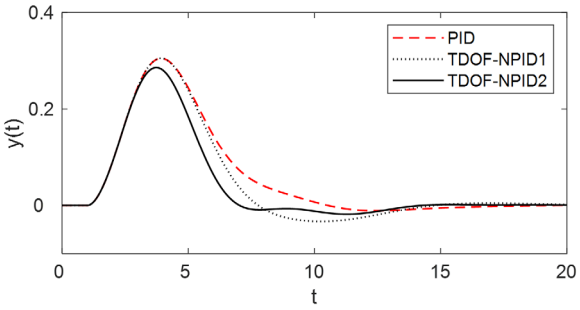

(b) Disturbance rejection

Figure 9. Responses of the three controllers for process 2 with c = 2.0

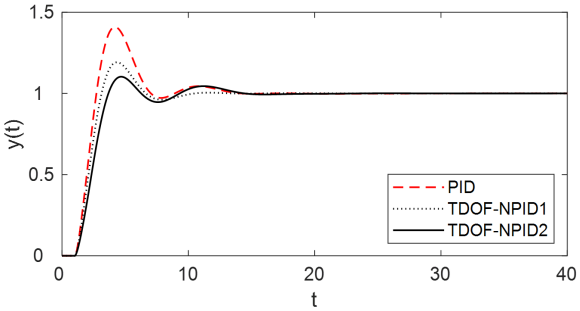

(a) Setpoint tracking

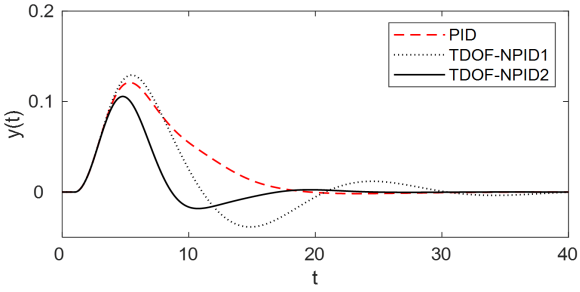

(b) Disturbance rejection

Figure 10. Responses of the three controllers for process 2 with c = 5.0

Table 4. Performance comparison for the three controllers for process 2

c	Controller	Setpoint tracking			Disturbance rejection		
		M_p	t_s	IAE_{SP}	M_{peak}	t_{rcy}	IAE_{DIS}
2	PID	32.404	5.169	2.476	0.305	9.439	1.221
	TDOF-NPID1	19.277	7.081	2.309	0.305	12.899	1.208
	TDOF-NPID2	9.648	9.239	2.409	0.286	12.257	0.945
5	PID	40.942	6.552	3.134	0.121	16.562	0.887
	TDOF-NPID1	19.186	6.050	2.609	0.129	27.783	1.024
	TDOF-NPID2	10.311	7.954	2.784	0.106	15.006	0.524

Table 4 demonstrates the effectiveness of the proposed methods in comparison with the PID controller. For c = 2, all the performance indices (M_p, M_{peak}, and IAE_{SP}) are lower for the proposed methods, except for t_s and t_{rcy}. For c = 5, the proposed methods outperform the PID controller in all aspects except for t_s. It's worth noting that the PID controller's overshoot (M_p) is significantly larger.

4.3 Case 3: Third-order Process

A third-order process with a positive zero is considered. The process parameter c has two distinct values, namely 1 and 2. This process is challenging to control because a higher value of c leads to a higher undershoot.

$$G_3(s) = \frac{1 - cs}{(1+s)^3}, \text{ c} = 1, 2 \tag{13}$$

Optimizations for the two values of c are achieved using the three controllers and the HGA. Table 5 details the settings for each controller.

Table 5. Tuned parameters for the three controllers for process 3

c	Controller	Parameters				
		K_p	K_i	K_d	α	β
1	PID	1.190	0.516	1.088		
	TDOF-NPID1	1.294	0.654	1.120	0.299	
	TDOF-NPID2	1.349	0.707	1.211	0.366	0.257
2	PID	0.701	0.280	0.618	-	-
	TDOF-NPID1	0.742	0.334	0.617	0.124	
	TDOF-NPID2	0.750	0.340	0.634	0.150	0.122

Figures 11 and 12 illustrate the setpoint tracking responses to unit step input and the disturbance rejection responses to unit step disturbance for the three controllers for process 3 and the two respective values of the parameter c, while Table 6 quantitatively compares the performance of the three controllers.

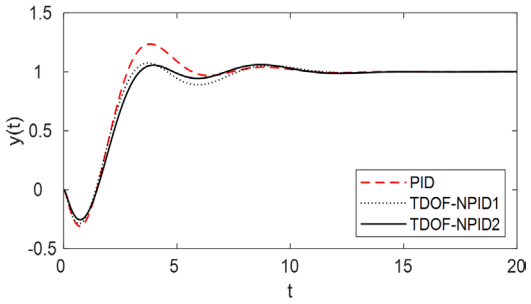

(a) Setpoint tracking

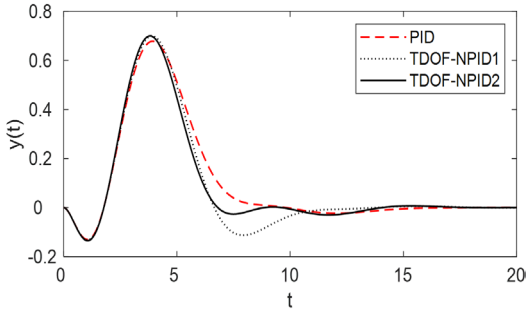

(b) Disturbance rejection

Figure 11. Responses of the three controllers for process 3 with c = 1.0

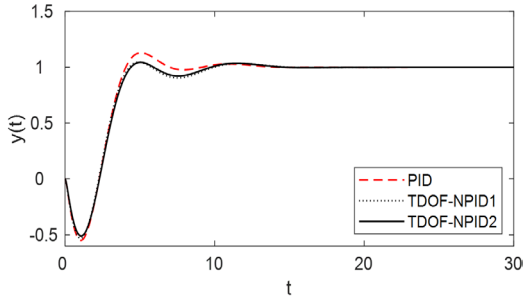

(a) Setpoint tracking

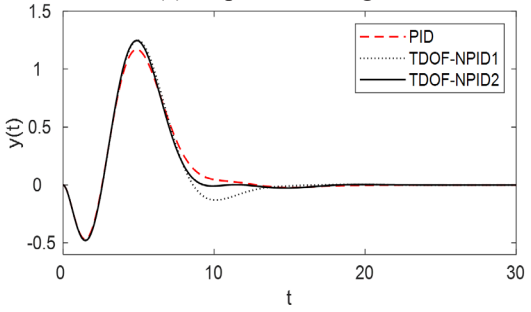

(b) Disturbance rejection

Figure 12. Responses of the three controllers for process 3 with c = 2.0

Table 6. Performance comparison for the three controllers for process 3

c	Controller	Setpoint tracking			Disturbance rejection		
		M_p	t_s	IAE_{SP}	M_{peak}	t_{rcy}	IAE_{DIS}
1	PID	23.607	5.153	2.912	0.678	7.608	2.367
	TDOF-NPID1	7.489	6.897	2.813	0.670	9.951	2.418
	TDOF-NPID2	6.051	3.105	2.810	0.699	6.506	2.176
2	PID	12.878	5.996	4.193	1.169	9.633	5.156
	TDOF-NPID1	4.485	8.387	4.212	1.248	12.084	5.411
	TDOF-NPID2	4.289	7.889	4.216	1.247	8.562	5.060

As shown in Figures 11 and 12 and in Table 6, for c = 1, the TDOF-NPID2 controller outperforms the PID controller for all performance indices except for M_{peak}. For c = 2, the TDOF-NPID2 controller also performs best for M_p, t_{rcy}, and IAE_d, except for t_s. However, IAE_{SP} and M_{peak} feature similar values for all the three methods. Notably, the PID controller features a very high M_p value, and despite having one less tuning parameter, the responses of the TDOF-NPID1 controller are similar to those of the TDOF-NPID2 controller.

4.4 Case 4: Nonlinear Sprott Circuit

A general model of the Sprott circuit is considered, which was built using just passive components (resistors and capacitors) and active components (diodes and inverting operational amplifiers) (Sprott, 2000; Rosas Almeida et al., 2006; Yau et al., 2011).

$$\dddot{x} + a\ddot{x} + \dot{x} = G_i(x) \tag{14}$$

where a is a constant and $G_i(x)$ belongs to the class of elementary piecewise functions. One function of $G_i(x)$ can be

$$G_i(x) = -1.2x + 2sgn(x) \tag{15}$$

where $sgn(\cdot)$ denotes the signum function.

Defining state variables as $x_1 = x$, $x_2 = \dot{x}$ and $x_3 = \ddot{x}$, and setting a = 0.6 gives a state space form (Sprott, 2000). For controlling this model, it is assumed that the control input u affects the second state equation (Yau et al., 2011), while a disturbance d impacts the third state equation:

$$\begin{aligned} \dot{x}_1 &= x_2 \\ \dot{x}_2 &= x_3 + u \\ \dot{x}_3 &= -1.2x_1 - x_2 - 0.6x_3 + 2\,\mathrm{sgn}(x_1) + d \\ y &= x_1 \end{aligned} \tag{16}$$

where y is the output. The control input u is considered to be limited to the input supply value of the operational amplifier.

Figure 13 depicts the Sprott circuit's chaotic behavior with $u = d = 0$ and $\boldsymbol{x}(0) = [-1,-2,1]^T$.

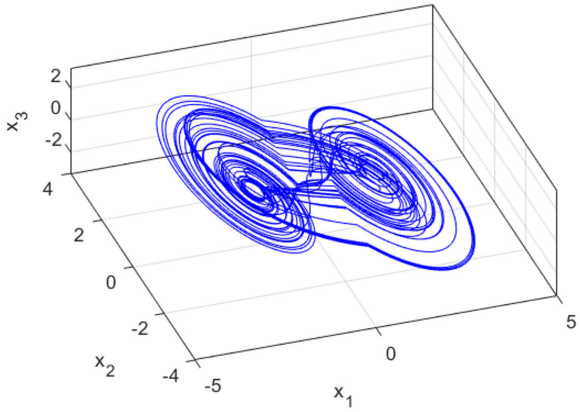

Figure 13. Sprott circuit's chaotic behavior

Table 7 shows the controller settings optimized by using the HGA.

In Figure 14, the setpoint tracking performances of the three controllers are compared for a unit step input. Additionally, the disturbance rejection performances are evaluated for a step disturbance of magnitude 3. It is assumed that the system starts from zero initial conditions. Table 8 shows the performance comparison for the three controllers.

Table 7. Tuned parameters of the three controllers for the nonlinear system

Controller	Parameters				
	K_p	K_i	K_d	α	β
PID	673.645	296.037	86.752	-	-
TDOF-NPID1	465.547	368.178	81.294	0.147	-
TDOF-NPID2	675.422	388.217	131.163	0.123	0.296

Table 8. Performance comparison for the three controllers for the nonlinear system

Controller	Setpoint tracking			Disturbance rejection		
	M_p	t_s	IAE_{SP}	M_{peak}	t_{rcv}	IAE_{DIS}
PID	46.794	0.886	0.497	0.008	11.204	0.039
TDOF-NPID1	4.096	0.415	0.263	0.008	8.216	0.032
TDOF-NPID2	0.024	0.542	0.279	0.007	9.511	0.030

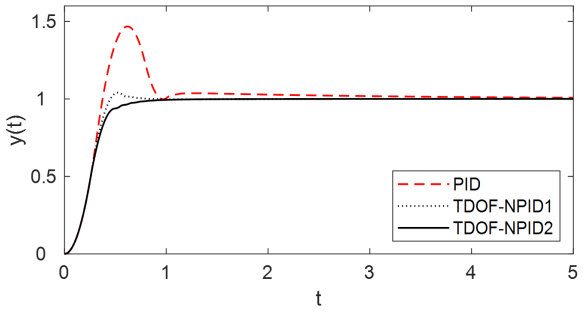

(a) Setpoint tracking

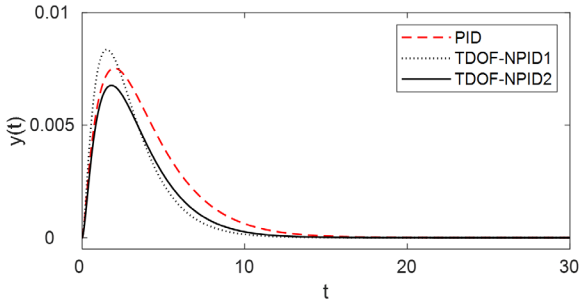

(b) Disturbance rejection

Figure 14. Responses of the three controllers for the nonlinear system.

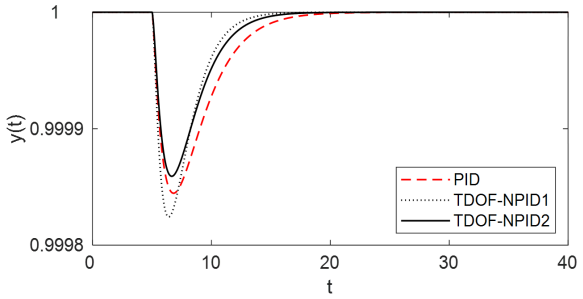

Figure 15. Responses of the three controllers for the case when a is increased (a = 0.6→0.72)

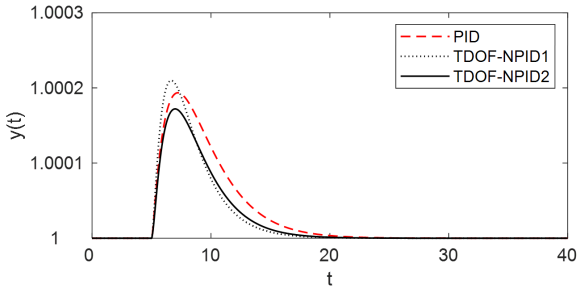

Figure 16. Responses of the three controllers for the case when a is decreased (a = 0.6→0.48)

The results in Figure 14 and Table 8 demonstrate that the proposed controllers outperform the PID controller. To that, the TDOF-NPID2 controller has the lowest M_p and M_{peak}. Notably, the TDOF-NPID1 controller achieves a similar performance to the TDOF-NPID2 controller except for M_p.

Additionally, the system's robustness to parameter variations was assessed by perturbing the parameter a by ± 20% of its nominal value of 0.6 at 5 seconds. Figures 15 and 16 depict the resulting responses for the case when a is increased (a = 0.6→0.72) and decreased (a = 0.6→0.48), respectively. Figures 15 and 16 demonstrate that parameter variations have a negligible impact on the response of all three methods.

Nevertheless, a closer examination of the quantitative results in Table 9 indicates that the proposed controllers feature a superior performance in comparison with the PID controller for most metrics, except for the M_{peak} of the TDOF-NPID1 controller.

5. Conclusion

This study introduced two TDOF NPID controllers which were designed to both follow a desired reference signal and reduce the impact of external influences. The proposed controllers included a linear P-type or PD-type feedforward

Table 9. Performance comparison of the three controllers in the context of parameter variations

Controller	a = 0.6→0.72			a = 0.6→0.48		
	M_{peak} (×10^{-3})	t_{rcv}	IAE (×10^{-3})	M_{peak} (×10^{-3})	t_{rcv}	IAE (×10^{-3})
PID	0.15537	15.4397	0.75065	0.1938	17.3791	1.1259
TDOF-NPID1	0.17573	12.3859	0.60357	0.2098	14.4812	0.9053
TDOF-NPID2	0.14086	13.7129	0.57241	0.1721	15.7315	0.8586

compensator within an NPID control framework to overcome the limitations of ODOF PID controllers. A hybrid genetic algorithm was also employed to achieve optimal controller settings. This approach minimized the total error over time, ensuring a superior performance as regards both setpoint tracking and disturbance rejection. A set of simulations was carried out for three processes with distinct parameter c values and one nonlinear system. The simulation results showed that the TDOF NPID controllers significantly reduced both the overshoot (M_p) and the integral absolute error (*IAE*) in comparison with the PID controller. Interestingly, while the TDOF-NPID2 controller achieved slightly better results than the TDOF-NPID1 controller, the difference was insignificant. Field engineers often struggle with controller tuning as the number of parameters increases. The TDOF structure, however, simplifies this process by allowing the independent tuning of parameters for both setpoint tracking and disturbance rejection. As such, while K_p, K_i, and K_d can be tuned for disturbance rejection, α and β can be tuned for optimizing setpoint tracking. Future research will focus on the stability analysis for TDOF NPID controllers and their practical implementation in real-world systems.

Acknowledgements

This paper was supported by the Education and Research promotion program of KOREATECH in 2026.

REFERENCES

Allagui, N. Y., Salem, F. A. & Aljuaid, A. M. (2021) Artificial Fuzzy-PID Gain Scheduling Algorithm Design for Motion Control in Differential Drive Mobile Robotic Platforms. *Computational Intelligence and Neuroscience*. 2021(2), 1-13. https://doi.org/10.1155/2021/ 554288.

Araki, M. (1984) PID control. In: Unbehauen, H. (ed.) *Control Systems, Robotics and Automation.* (vol. II). Oxford, UK, Eolss Publishers Co. Ltd.

Araki, M. & Taguchi, H. (2003) Two-Degree-of-Freedom PID Controllers. *International Journal of Control, Automation, and Systems*. 1(4), 401-411. https://doi.org/10.11509/isciesci.42.1_18.

Åström, K. J., Panagopoulos, H. & Hägglund, T. (1998) Design of PI Controllers based on Non-Convex Optimization. *Automatica*. 34(5), 585-601. https://doi.org/10.1016/S0005-1098(98)00011-9.

Chen, D. & Seborg, D. E. (2002) PI/PID Controller Design Based on Direct Synthesis and Disturbance Rejection. *Industrial & Engineering Chemistry Research.* 41(19), 4807-4822. https://doi: 10.1021/ie010756m.

Chen, J. P., Lu, B. C., Fan, F. et al. (2011) A Nonlinear PID Controller for Electro-Hydraulic Servo System Based on PSO Algorithm. *Applied Mechanics and Materials.* 141, 157-161. https://doi.org/10.4028/www.scientific.net/AMM.141.157.

Deb, K., Pratap, A., Agarwal, S. et al. (2002) A Fast and Elitist Multiobjective Genetic Algorithm: NSGA-II *IEEE Transactions on Evolutionary Computation.* 6(2), 182-197. https://doi.org/10.1109/4235.996017.

Goh, J., Adepu, S., Tan, M. et al. (2017) Anomaly Detection in Cyber Physical Systems Using Recurrent Neural Networks. In: *IEEE 18th International Symposium on High Assurance Systems Engineering (HASE)*, *12-14 January 2017, Singapore*. pp. 140-145.

Hasan, M. W. & Abbas, N. H. (2022) An Adaptive Nonlinear PID Design for 6-DOF Underwater Robotic Vehicle. *Advances in Electrical and Electronic Engineering*. 20(2), 193-203. https://doi.org/10.15598/aeee. v20i2.4370.

Jiang, F. & Gao, Z. (2001) An application of nonlinear PID control to a class of truck ABS problems. In: *Proceedings of the 40th IEEE Conference on Decision and Control*, *4-7 December 2001*, *Orlando, USA*. New York, USA, IEEE. pp. 516-521.

Jin, G.-G. & Son, Y.-D. (2019) Design of a Nonlinear PID Controller and Tuning Rules for First-Order Plus Time Delay Models. *Studies in Informatics and Control*. 28(2), 157-166. https://doi.org/10.24846/v28i2y201904.

Jin, G.-G. & Jarso, A. K. (2024) An improved hybrid genetic algorithm using the affine combination-based reproduction. *Communications in Statistics - Simulation and Computation.* 1, 1-27. https://doi.org/10.1080/03610918.2024.2363958.

Mahmooddabadi, M. J., Taherkhorsandi, M., Talebipour, M. et al. (2014) Adaptive robust PID control subject to supervisory decoupled sliding mode control based upon genetic algorithm optimization. *Transactions of the Institute of Measurement and Control*. 37(4), 505-514. https://doi.org/10.1177/0142331214543295.

Pathiran A. R. (2019) Improving the Regulatory Response of PID Controller Using Internal Model Control Principles. *International Journal of Control Science and Engineering.* 9(1), 9-14. https://doi.org/10.5923/j.control.20190901.02.

Raja, G. L. & Ali, A. (2021) Enhanced tuning of Smith predictor based series cascaded control structure for integrating processes. *ISA Transactions.* 114, 191-205. https://doi.org/10.1016/j.isatra.2020.12.045.

Rosas Almeida, D. I., Alvarez., J. & Barajas, J. G. (2006) Robust synchronization of Sprott circuits using sliding mode control. *Chaos, Solitons & Fractals.* 30(1), 11-18. https://doi.org/10.1016/j.chaos.2005.09. 011.

Santos, M. A. & Raffo, G. V. (2016) Path tracking Model Predictive Control of a Tilt-rotor UAV carrying a suspended load. In: *19th International Conference on Intelligent Transportation Systems (ITSC), 1-4 November 2016*, *Rio de Janeiro, Brazil*. New York, USA, IEEE. pp. 1458-1463.

Santosh Kumar, D. B. & Padma Sree, R. (2016) Tuning of IMC based PID controllers for integrating systems with time delay. *ISA Transactions.* 63, 242-255. https://doi.org/10.1016/j.isatra.2016.03.020.

Seraji, H. (1998) A New Class of Nonlinear PID Controllers for Robotic Applications. *Journal of Field Robotics*. 15(3), 161-181. https://doi.org/10.1002/(SICI)1097-4563(199803)15:3%3c161::AID-ROB4%3e3.0.CO;2-ODigital Object Identifier (DOI).

Shamsuzzoha, M. (2013) Closed-Loop PI/PID Controller Tuning for Stable and Integrating Process with Time Delay. *Industrial & Engineering Chemistry Research.* 52(36), 12973-12992. https://doi.org/10.1021/ie401808m.

So, G.-B. (2022) Design of Linear PID Controller for Pure Integrating Systems with Time Delay Using Direct Synthesis Method. *Processes.* 10(5), art. ID 831. https://doi.org/10.3390/pr10050831.

Sprott, J. C. (2000) A New Class of Chaotic Circuit. *Physics Letters A*. 266(1), 19-23. https://doi.org/10.1016/ S0375-9601(00)00026-8.

Sun, X., Liu, N., Shen, R. et al. (2022) Nonlinear PID Controller Parameters Optimization Using Improved Particle Swarm Optimization Algorithm for the CNC System. *Applied Sciences.* 12(20), art. ID 10269. https://doi.org/10.3390/app122010269.

Sundari, S. & Nachiappan, A. (2018) Design of optimal Linear Quadratic Regulator for the stabilization of Continuous Stirred Tank Reactor(CSTR) Process. *International Journal of Pure and Applied Mathematics.* 118(24), 1-19.

Veronesi, M. & Visioli, A. (2023) Optimized tuning rules for proportional-integral controllers with selected robustness. *Asian Journal of Control*. 25(3), 1731-1744. https://doi.org/10.1002/asjc.2888.

Wang, H., Wu, Z & Liu, Y. et al. (2009) Space transformation search: A new evolutionary technique. In: *GEC '09: Proceedings of the first ACM/SIGEVO Summit on Genetic and Evolutionary Computation*, *12-14 June 2009, Shanghai, China.* New Yok, USA, Association for Computing Machinery. pp. 537-544.

Wu, Z., Li, D. & Xue, Y. (2016) A New PID Controller Design with Constraints on Relative Delay Margin for First-Order Plus Dead-Time Systems. *Processes*. 7(10), art. ID 713. https://doi.org/10.3390/pr7100713.

Yau, H.-T., Pu, Y-C. & Li, S. C. (2011) An FPGA-Based PID Controller Design for Chaos Synchronization by Evolutionary Programming. *Discrete Dynamics in Nature and Society*. 2011, art. ID 516031. https://doi.org/10.1155/2011/516031.

Zhang, H. & Hu, B. (2012) The Application of Nonlinear PID Controller in Generator Excitation System. *Energy Procedia.* 17(A), 202-207. https://doi.org/10.1016/ j.egypro.2012.02.084.

Zou, H. & Li, H. (2015) Tuning of PI–PD controller using extended non-minimal state space model predictive control for the stabilized gasoline vapor pressure in a stabilized tower. *Chemometrics and Intelligent Laboratory Systems.* 142, 1-8. https://doi.org/10.1016/j.chemolab.2014.12.012.